Selective Removal of Metallic Single-walled Carbon Nanotubes by Microwave-assisted Treatment of Nitronium Ions

Journal:	*Journal of Materials Chemistry A*
Manuscript ID:	TA-ART-04-2014-001816.R1
Article Type:	Paper
Date Submitted by the Author:	10-May-2014
Complete List of Authors:	Shen, Xiao; University of Shanghai for Science and Technology, Qiu, Hanxun; University of Shanghai for Science and Technology, School of Materials Science and Engineering Li, Jing; University of Shanghai for Science and Technology, School of Materials Science and Engineering Zhang, Huijuang; University of Shanghai for Science and Technology, School of Materials Science and Engineering Zhao, Bin; University of Shanghai for Science and Technology, School of Materials Science and Engineering Yang, Junhe; University of Shanghai for Science and Technology, School of Materials Science and Engineering

Selective Removal of Metallic Single-walled Carbon Nanotubes by Microwave-assisted Treatment of Nitronium Ions

Xiao Shen, Hanxun Qiu*, Jing Li, Huijuan Zhang, Bin Zhao, Junhe Yang*

School of Materials Science and Engineering, University of Shanghai for Science and Technology, Shanghai 200093, P. R. China

Corresponding Author: Hanxun Qiu; Junhe Yang
E-mail: hxqiu@usst.edu.cn; jhyang@usst.edu.cn
Tel & Fax: +86-21-55271723

Abstract:

A facile and rapid technique for selective removal of metallic single-walled carbon nanotubes (M-SWCNTs) was developed by microwave-assisted treatment of nitronium ions. Upon exposure to microwave, M-SWCNTs homogeneously dispersed in organic solution were prone to reacting with an electron acceptor reagent-positively charged nitronium ions as compared to their counterpart semiconducting (S-) SWCNTs. The well functionalized M-SWCNTs were just separated and removed from residual S-SWCNTs by standing the suspension. The resulting material contained highly enriched S-SWCNTs of which the proportion increased from approximate 62 mol% in as-received SWCNTs to nearly 90 mol%. The effectiveness of removing M-SWCNTs was confirmed by the resonant Raman spectra and UV-vis-NIR absorption spectra. The microwave-enhanced separation mechanism was discussed as well.

1 Introduction

Single-walled carbon nanotubes (SWCNTs) have been greatly attracting the scientific community because of the unique electronic properties and promising applications,[1-3] particularly, of semiconducting single-walled carbon nanotubes (S-SWCNTs).[4-9] However, the as-prepared SWCNTs either experimentally or commercially used naturally contain two different species of nanotubes, namely the S-SWCNTs and the metallic SWCNTs (M-SWCNTs). As a matter of fact, pure S-SWCNTs excluding any M-SWCNTs have never been obtained directly by any synthetic techniques explored so far. This extremely hinders the further study of carbon nanotubes, and especially limits the applications for promising nanocarbon-based electronics which are widely believed to be the best candidates to surpass modern silicon devices in many areas. It's therefore imperative to separate or enrich semiconducting nanotubes before integrating them into electronic devices. Recently tremendous efforts have particularly been undertaken and focused on researching more efficient separation techniques with the aim of achieving SWCNTs of a single type, especially s-SWCNTs because of the considerable superiority as potential novel materials.[10,11] In general, these techniques succeeded in realizing the separation on the basis of the tiny differences in structures and properties between two kinds of nanotubes. These demonstrated post-growth techniques for separating SWCNTs primarily include dielectrophoresis,[12] ultracentrifugation,[13] DNA wrapping chromatography,[14] selective oxidation,[15,16] light induced oxidation,[17] selective chemistry,[18-20] gel chromatography,[21] and microwave-assisted irradiation[22,23] and so on. Although these developed techniques exhibit perceivable effectiveness in enriching carbon nanotubes of a certain type, they suffer from problems and limitations, such as low yield, high cost, inapplicability in large scale, and intricate operating processing. Therefore, to pursue a more promising and efficient approach remains attracting researchers great attention.

Due to its advantages, including a higher throughput, greater penetration depth of heat into material, lower power costs and selective heating within the material over conventional chemical approaches of heating,[24] microwave-assisted technique was recently introduced into carbon nanotube (CNT) chemistry, by which products with a high yield and purity resulting from a rapid reaction rate and a small amount of use of solvent have been obtained.[25] As a kind of high-power wave located between infrared and radio frequency range in electromagnetic spectrum, microwave irradiation has exhibited its advantages in treating CNTs. When CNTs are exposed to microwaves, strong absorption are observed producing intense heating, outgassing, and light emission.[26]

The interaction of microwave with CNTs opens the door to preferentially treat CNTs with special structures. Our group recently developed a technique that involved the microwave irradiation on homogeneously dispersed SWCNTs in mixed acids.[23-27] It proved an highly efficient approach to enrich S-SWCNTs by selectively removing M-SWCNTs. Although the mechanism of CNT-microwave interaction remains incompletely understood, it is believed that microwaves plays a crucial role on discriminating two types of SWCNTs. Since corrosive acidic reagents were commonly used in the process, it may cause environmental pollution and raise operating risks. To overcome this adverse problem, we here demonstrate an improved route to efficient enrichment of S-SWCNTs, which was briefly performed through microwave-irradiating the highly dispersed suspension of SWCNTs-nitronium ions (NO^{2+}). As both microwave irradiation and NO^{2+} tended to preferentially attack M-SWCNTs induced by the abundant presence of electron density at the Fermi level, the synergistic effect of microwave and NO^{2+} make it efficient to selectively remove M-SWCNTs, and accordingly S-SWCNTs could be enriched. This promising technique is expected to speed up the pace of exploiting carbon nanotubes for fabrication of nanotube-based electronics.

2 Experimental Section

2.1 Microwave irradiation and reaction

The reaction was performed in a single-mode CEM Discover microwave system (500 W, 2450 MHz). Experimental parameters, including irradiation power, reaction temperature inside the vessel were precisely controlled by connecting to a computer. The starting SWCNTs prepared by the high-pressure carbon monoxide chemical vapor deposition method (HiPCO) were obtained commercially from Carbon Nanotechnologies, Inc. Chemical reagents were purchased from Sinolpharm Chemical Reagent Co., Ltd. And all of them were used as received, unless otherwise stated. In a typical reaction, nitronium tetrafluoroborate (NO_2BF_4, NTFB) of 5 mmol was dissolved in TMS/ chloroform (1:1 by weight) solution of 10 mL. The nitronium salts were ionized in the mixed solvent as the following equation:

$$NO_2BF_4 \longrightarrow NO_2^+ + BF_4^- \qquad (1)$$

Subsequently, 1 mg of the pristine SWCNTs were added into a flask containing 10 mL of the aforementioned nitronium solution. The solution was ultrasonicated for 10 min at room temperature to ensure the SWCNTs were well dispersed. Then the flask loading the solution was subject to microwave irradiation in the microwave system for 2h at the temperature of 60 °C. After reaction, the suspension was placed for a few hours, then the supernatant was removed. The residual was washed with deionized water a few times until any remaining absorbate attached onto the surface of carbon nanotubes were completely eliminated. Freeze-drying was successively carried out to obtain SWCNTs powder. As a final step, thermal annealing treatments were conducted at 1000 °C under Ar atmosphere for 30 min to integrate carbon nanotubes. Hereto, the samples were prepared for characterization measurements as discussed below.

2.2 Characterizations

Raman spectra for carbon nanotubes were recorded using spectrophotometers with laser excitations of 514.5 and 632.8 nm (Renishaw, inVia plus), and 785 nm (Perkin Elmer, Raman Station 400F). The solution-phase optical absorption data of SWCNTs dispersed in 0.5% aqueous solution of SDBS were recorded using a UV-Vis Spectrometer (Lambda 750S) with a 10-mm path length Pyrex cell. Scanning electron microscope (SEM) observations were conducted using a field emission electron microscope (accelerating voltage, 5.0 kV; beam current, 10 μA, JEOL S-4800) by fixing specimens to the sample holder with a piece of adhesive carbon tape

3 Results and Discussions

3.1 Raman spectra investigation-RBMs analysis

To determine changes especially in chirality of SWCNTs, Raman scattering serves as one of the most powerful tools by which both the chirality-dependent resonance radial-breathing modes (RBMs) located at lower frequencies and the tangential mode (G-band) at a higher frequency can provide significant evidence on characteristics of nanotubes.[28,29] According to the correlation between frequencies of RBMs and tube diameters, it is well known that lower RBMs correspond to larger diameter SWCNTs, and that the higher ones to smaller diameter SWCNTs. By the equation of [$\omega(\mathrm{cm}^{-1})=235/d(\mathrm{nm})+9$], the diameters corresponding to each RBM have been identified and labeled in Fig. 1. Moreover, the chirality-dependent resonance-RBM throws light on whether the carbon nanotubes are metallic or semiconducting according to the theoretical illustration of the well known Kataura plots.[29,30] RBMs corresponding to energy transitions, typically the first transition of S-SWNTs (S_{11}), the second (S_{22}), and the first metallic transition (M_{11}) between pairs of van Hove singularities in the density of states of CNTs, can be probed by Raman spectroscopy with the appropriate laser excitation energies.

The RBM bands representing either M- or S-SWCNTs were squarely dotted in the Raman spectra as shown in Fig. 1, respectively. It’s worth noting that all spectra have been normalized based on the intensity of G-band. Fig. 1A presents RBMs of the

Raman spectra for pristine and resultant materials, as measured using laser excitation of 514.5 nm. Peaks located around 220-300 cm^{-1} identified in the spectrum for pristine (black curve) are originated from M-SWCNTs. Noting that no SWCNTs including both the metallic- and semiconducting ones larger than 1.0 nm can be preferentially probed with the excitation energy of 514.5 nm for this batch of HiPCO tubes having diameters of 0.7-1.2 nm. Interestingly, it can be seen that the features of these peaks vanished even without trace after microwave treatment in the spectrum colored in red, suggesting no M-SWCNTs were probed in the resulting materials. To obtain pure carbon nanotubes, high temperature annealing treatment was carried out to eliminate any chemicals physically or chemically adsorbed onto the surface of tubes. Though peaks corresponding to M-SWCNTs with diameters of 1.0 and 0.94 nm seem slightly recovered after annealing (shown in blue), they are intensively weakened, indicating the fraction of M-SWCNTs with diameters of 0.78-1.0 nm in the resulting material was significantly reduced. Since the energy transitions between the van Hove singularities of the density of states are discrete, and nanotubes with special chirality and diameter can be only probed by certain excitation energy, it is essential to demonstrate the changes using Raman spectra measured at more than one laser excitations. Fig. 1B displays the Raman spectrum measured with wavelength of 785 nm. Both the typical peaks located at 201, 212, 222, 230 and 264 cm^{-1} and their corresponding diameters are labeled in the figure. Just quite differing from the case of spectra measured at 514.5 nm excitation, only S_{22} bands of S-SWCNTs ranging from 0.9 to 1.2 nm are in resonance around 180-300 cm^{-1}. Whereas all M-SWCNTs and part of small S-SWCNTs can't be probed. In comparison with Fig. 1A, the NTFB-treated materials exhibits similar RBMs as the pristine nanotubes, except for the slight depression and up-shifting of features in Fig. 1B. This slight blue-shift is expected to result from the interaction between physically adsorbed nitronium ions and π-system in carbon six-rings of S-SWCNTs. As this kind of physical adsorption with weak binding energy is generally not so strong as to destroy the chemical structure of nanotubes during adsorption and desorption processes, the features of S-SWCNTs could be fully recovered after annealing with almost same intensity ratios and peak positions as the pristine, as shown in the figure. It suggests the microwave-NTFB treatment doesn't make evident change on S-SWCNTs, especially those with large diameters. Fig. 1C shows the RBMs measured at excitation of 633nm. In this case, the metallic and semiconducting types of nanotubes are theoretically in resonance around 180-240 cm^{-1} and 240-300 cm^{-1}, respectively. Therefore the metallic bands at 191 cm^{-1} and 216 cm^{-1} corresponding to diameters of 1.29 and 1.14 nm and the semiconducting bands at 255 cm^{-1}, 282 cm^{-1} and 295 cm^{-1} corresponding to 0.95, 0.86 and 0.82 nm are simultaneously probed, as shown in the spectrum of pristine sample. In other words, the M-SWCNTs smaller than 1.14 nm and S-SWCNTs larger that 0.95 nm can hardly be in resonance by the laser excitation of 633 nm. In the spectra of treated sample, it can be noticed that features from the small diameter (0.86 nm and 0.82 nm) S-SWCNTs are greatly weakened, and never get recovered even after heat treatment. This may be attributed to the relatively large strain of small tubes which are more easily chemically attacked by nitronium ions. Moreover, features of metallic nanotubes with diameters of larger than 1.1 nm appear little change, as may be explained by their weak chemical reactivity with nitronium ions induced by high curvature radius. This result seems inconsistent with those from the Fig. 1A and B. However, as a matter of fact, they are complementary by each other and confirm the effectiveness of the proposed approach on separating SWCNTs of different types. The sufficient supports from Raman data demonstrate that the proposed approach is not only capable of selectively removing nearly all M-SWCNTs excluding large ones, but also make the diameter distribution of S-SWCNTs well narrowed.

3.2 Raman spectra investigation-G band analysis

Additionally, the removal of M-SWCNTs or the enrichment of S-SWNTs has been further evidenced by the line shape changes of G-bands in the Raman spectra both for the pristine and the annealed samples, as shown in Fig. 2. The broad and asymmetric G-band described as a Breit-Wigner-Fano (BWF) line shape located around 1540 cm^{-1} is believed to be characteristic that originates from the electron–phonon interactions in M-SWNTs.[28,31] By contrast, the BWF feature for the pristine SWNTs in Fig. 2A (black line) becomes absent from the treated sample (red line). A much narrower and symmetric G-band for the treated sample is present instead. As shown in Fig. 2B, the G band of the pristine SWCNTs is fitted with four semiconducting Lorentzian lines (centered at 1545, 1564, 1583, and 1590 cm^{-1}) and two broad, asymmetric metallic BWF lines (1515 and 1605 cm^{-1}). However, the latter two BWF peaks assigned to M-SWCNTs completely disappear and the semiconducting peaks almost remain unchanged for the treated sample (Fig. 2C), suggesting little M-SWCNTs contained in resulting materials. Moreover, the intensity ratios of G/D bands (Fig. 2A) for the pristine and NTFB-HTT treated SWCNTs are ~ 6.4 and 6.6, respectively, suggesting that the resulting SWCNTs after microwave-assisted NTFB-HTT treatments are still in high purity and their structure retain well.

3.3 Absorption spectra investigation

Optical absorption spectroscopy, another characterization tool as important as Raman spectroscopy, may provide valuable information on electronic states of both M-SWCNTs and S-SWCNTs.[32-34] UV-vis-NIR absorption spectra were measured to analyze the electronic states of the pristine and the annealed SWNTs. Fig. 3A presents comparatively the UV-vis-NIR absorption spectra of the pristine (black curve) and the annealed materials (marked with NTFB-HTT). In accordance with previous reports, it displays the energy transitions between pairs of van Hove singularities in the density of states of, typically S_{11} around 900-1500 nm, S_{22} from 630 to 900 nm, and M_{11} from 450 to 630 nm.[30] For the pristine SWCNTs, both the S-SWCNTs related bands (S_{11} and S_{22}) and metallic band (M_{11}) are observed, while the features of the M_{11} band becomes unclear and almost disappears for the NTFB-HTT material, suggesting the majority of M-SWCNTs were removed by microwave-assisted nitronium ions treatment. According to theoretical calculation, the fraction of M-SWCNTs in the materials can be quantitatively evaluated by the ratio of M_{11} band's area to the total areas of M_{11} and S_{22} bands, which is denoted as $M_{11} / (M_{11} + S_{22})$.[35] Fig. 3B presents the Lorentzian curve fitted M_{11} and S_{22} bands in the baseline-subtracted UV-vis-NIR spectrum for the pristine sample. The value of $M_{11} / (M_{11} + S_{22})$ is 0.38, consistent with the theoretical value of one third M-SWCNTs in the as-prepared materials. As predicted, the fraction of M-SWCNTs is greatly reduced to less than 0.13 % after the NTFB treatment followed by thermal annealing (Fig. 3C), and that of S-SWCNTs correspondingly gets closed to 90 %. It further confirms that the treatment integrating microwave irradiating and nitronium ions attack may efficiently remove M-SWCNTs. This results accord well with Raman spectra discussed above.

3.4 Morphology of SWCNTs

Fig. 4 presents typical SEM images of the pristine (Fig. 4A) and NTFB-treated SWCNTs (Fig. 4B), both of which were observed at the same magnification for a better comparison. As shown, the morphology of SWCNTs after treatment remains similar as that of the pristine SWCNTs, indicating the obtained SWCNTs possess good chemical structure and properties.

3.5 Mechanism discussion

As for the deep understanding of separation mechanism of the proposed approach, we believe the application of microwave plays a crucial role on efficiently sorting S-SWCNTs out from their counterparts. As well known, microwave heating has distinctive advantages over conventional methods, particularly including greater penetration depth of heat into material and selective heating within the material. The recent theoretical and experimental studies revealed that microwave-induced heating of carbon nanotubes might succeed through transformation of electromagnetic energy into mechanical vibrations.[36,37] When CNTs were exposed to intense microwaves in the range of 2-20 GHz, they would be transversely or longitudinally polarized depending on the specific resonance parameter, κ, which plays a key role in determining the behavior of CNTs. Typically, the dynamical response of CNTs to microwaves results in two effects, electron-phonon scattering (Joule heating) and the phonon-phonon scattering of which the energy transfer far exceeds the Joule heating. For SWCNTs with a different resonance parameter, the electron-phonon interaction or phonon-phonon interaction may dominate during energy transfer. This indicates that the efficiency of energy transfer from microwave to CNTs may be strongly dependent on the chemical structure and chirality of SWCNTs. M-SWCNTs, due to the abundance of charge density at Fermi level, would be much easier to be excited than S-SWCNTs. The strong electron-phonon or phonon-phonon interaction, thus made M-SWCNTs receive microwave energy more efficiently and have higher temperature than S-SWCNTs, as largely promotes the reactivity of M-SWCNTs. On the other hand, the tiny structure difference between metallic- and semiconducting- nanotubes endows them with distinct chemical reactivity. M-SWCNTs are prone to donating their electrons to form stable covalent bonds with an electron acceptor, as has been proved by previous reports.[18-20] Therefore, in the case of the proposed separation approach, the application of microwave, instead of using the conventional heating method, enlarged the difference in chemical reactivity among CNTs and greatly enhanced the selectivity and efficiency of reaction with nitronium ions. The synergistic effect of microwave irradiation and good electron acceptor, nitronium ions, made M-SWCNTs be covalently functionalized while retained S-SWCNTs nearly intact. Since the functionalized M-SWCNTs have much better dispersivity than S-SWCNTs, they can be easily separated from the easily agglomerated S-SWCNTs by standing the suspension and removing the upper supernatant. Though the large M-SWCNTs, due to the relatively low chemical reactivity induced by high curvature radius, seem not be completely removed, as is in accordance with what reported previously, the approach exhibits its high efficiency and simplicity in separating CNTs over the reported techniques.

4 Conclusion

In summary, a microwave-assisted treatment of as-prepared HiPCO SWCNTs that are well dispersed in NTFB solution has proven to be an effective method for enriching S-SWCNTs with a narrow diameter distribution by preferentially eliminating M-SWCNTs and S-SWCNTs with small diameters. The proportion of S-SWCNTs contained in resulting materials is increased to approximate 90 mol% from around 62 mol% in the as-received samples. More importantly, the morphology and structure of the obtained S-SWCNTs are well preserved, ensuring the intrinsic semiconducting properties of S-SWCNTs which is vital for fabricating intriguing nanoscale devices. Compared to the reported techniques, the proposed microwave-induced approach shows advantages of high efficiency, environment-friendliness, and the simultaneous selectivity on diameter and electrical property of SWCNTs. The enriched S-SWCNTs with intrinsic semiconducting properties and desirable tube diameters will be promising for fabricating the potential SWCNT-based electronic devices.

Acknowledgments

The authors are grateful to NSFC (51102167, U1260104), Shanghai Pujiang Talent Program (11PJ1407200), and Innovation Program of Shanghai Municipal Education Commission (12YZ101, 13ZR1429000, slg11026).

References

1 S. J. Tans, A. R. M. Verschueren and C. Dekker, *Nature*, 1998, **393,** 49-52.

2 V. Sgobba and D. M. Guldi, *Chem. Soc. Rev.*, 2009, **38,** 165-184.

3 M. Barkelid and V. Zwiller, *Nat. Photonics.*, 2014, **8,** 47-51.

4 C. Wang, A. Badmaev, A. Jooyaie, M. Bao, K. L. Wang, K. Galatsis, and C. Zhou, *ACS Nano*, 2011, **5,** 4169-4176.

5 C. Wang, J. C. Chien, K. Takei, T. Takahashi, J. Nah, A. M. Niknejad, and A. Javey, *Nano Lett.,* 2012, **12,** 1527-1533.

6 H. Ryu, D. Kalblein, R. T. Weitz, F. Ante, U. Zschieschang, K. Kern, O. G. Schmidt and H. Klauk, *Nanotechnology,* 2010, **21,** 475207.

7 W. S. Li, P. X. Hou, C. Liu, D. M. Sun, J. T. Yuan, S. Y. Zhao, L. C. Yin, H. T. Cong and H. M. Cheng, *ACS Nano*, 2013, **7,** 6831-6839.

8 T. DeBorde, L. Aspitarte, T. Sharf, J. W. Kevek and E. D. Minot, *ACS Nano*, 2014, **8,** 216-221.

9 W. Xu, J. W. Zhao, L. Qian, X. Y. Han, L. Z. Wu, W. C. Wu, M. Song, L. Zhou, W. M. Su, C. Wang, S. H. Nie and Z. Cui, *Nanoscale*, 2014, **6,** 1589-1595.

10 H. L. Zhang, B. Wu, W. P. Hu and Y. Q. Liu, *Chem. Soc. Rev.*, 2011, **40,** 1324-1336.

11 H. X. Qiu, Y. X. Zheng and J. H. Yang, *New Carbon Materials*, 2012, **27,** 1-11.

12 R. Krupke, F. Hennrich, H. V. Lohneysen, and M. M. Kappes, *Science, 2003,* **301,** 344-347.

13 M. S. Arnold, A. A. Green, J. F. Hulvat, S. I. Stupp and M. C. Hersam, *Nat. Nanotech.,* 2006, **1,** 60-65.

14 M. Zheng, A. Jagota, E. D. Semke, B. A. Diner, R. S. Mclean, S. R. Lustig, R. E. Richardson and N. G. Tassi, *Nat. Mater.*, 2003, **2,** 338-342.

15 G. Zhang, P. Qi, X. Wang, Y. R. Lu, X. L. Li, R. Tu, S. Bangsaruntip, D. Mann, L. Zhang and H. J. Dai, *Science*, 2006, **314,** 974-977.

16 **A.** Anson-Casaos, M. Gonzalez, J. Gonzalez-Dominguez, and M. Martinez, *Langmuir*, 2011, 27, 7192-7198.

17 M. Mahjouri-Samani, Y. S. Zhou, W. Xiong, Y. Gao, M. Mitchell and Y. F. Lu, *Nanotechnology*, 2009, **20,** 495202.

18 Y. Maeda, S. I. Kimura, M. Kanda, Y. Hirashima, T. Hasegawa, T. Wakahara, Y. F. Lian, T. Nakahodo, T. Tsuchiya, T. Akasaka, J. Lu, X. W. Zhang, Z. X. Gao, Y. P. Yu, S. Nagase, S. Kazaoui, N. Minami, T. Shimizu, H. Tokumoto and R. Saito, *J. Am. Chem. Soc.,* 2005, **127,** 10287-10290.

19 K. H. An, J. S. Park, C. M. Yang, S. Y. Jeong, S. C. Lim, C. Kang, J. H. Son, M. S. Jeong and Y. H. Lee, *J. Am. Chem. Soc.*, 2005, **127,** 5196-5203.

20 A. K. Sundramoorthy, S. Mesgari, J. Wang, R. Kumar, M. A. Sk, S. H. Yeap, Q. Zhang, S. K. Sze, K. H. Lim and M. B. Chan-Park, *J. Am. Chem. Soc.*, 2013, **135,** 5569-5581.

21 T. Tanaka, H. Jin, Y. Miyata, S. Fujii, H. Suga, Y. Naitoh, T. Minari, T. Miyadera, K. Tsukahoshi and H. Kataura, *Nano Lett.*, 2009, **9,** 1497-1500.

22 H. C. Shim, J. W. Song, Y. K. Kwak, S. Kim and C. S. Han, *Nanotechnology*, 2009, **20,** 065707.

23 H. Qiu, Y. Maeda and T. Akasaka, *J. Am. Chem. Soc.*, 2009, **131,** 16529-16533.

24 A. C. Metaxas and R. J. Meredith, Industrial microwave heating, IET, 1983.

25 F. G. Brunetti, M. A. Herrero, J. D. M. Munoz, A. Diaz-Ortiz, J. Alfonsi, M. Meneghetti, M. Prato and E. Vázquez, *J. Am. Chem. Soc.*, 2008, *130*, 8094-8100.

26 E. Vazquez and M. Prato, *ACS Nano,* 2009, **3,** 3819-3824.

27 H. Qiu, Y. Maeda, T. Akasaka and J. Yang, *Sep. Purif. Technol.*, 2012, **96,** 182-186.

28 M. S. Dresselhaus, G. Dresselhaus, A. Jorio, A. G. Souza Filho and R. Saito, *Carbon*, 2002, **40,** 2043-2061.

29 H. Kataura, Y. Kumazawa, Y. Maniwa, I. Umezu, S. Suzuki, Y. Ohtsuka and Y. Achiba, *Synth. Met.*, 1999, **103,** 2555-2558.

30 R. B. Weisman and S. M. Bachilo, *Nano Lett*., 2003, **3,** 1235-1238.

31 S. D. M. Brown, A. Jorio, P. Corio, M. S. Dresselhaus, G. Dresselhaus, R. Saito, and K. Kneipp, *Phys. Rev. B*, 2001, **63,** 155414.

32 R. Matsunaga, K. Matsuda and Y. Kanemitsu, *Phys. Rev. Lett.*, 2011, **106,** 037404.

33 G. A. Rance, D. H. Marsh, R. J. Nicholas and A. N. Khlobystov, *Chem. Phys. Lett.*, 2010, **493,** 19-23.

34 W. J. Kim, C. Y. Lee, K. P. O'brien, J. J. Plombon, J. M. Blackwell and M. S. Strano, *J. Am. Chem. Soc.*, 2009, **131,** 3128-3129.

35 B. R. Priya and H. J. Byrne, *J. Phys. Chem. C*, 2009, **113,** 7134-7138.

36 Z. Ye, W. D. Deering, A. Krokhin, and J. A. Roberts. *Phys. Rev. B*, 2006, **74,** 075425.

37 K. R. Paton and A. H. Windle, *Carbon*, 2008, **46,** 1935-1941.

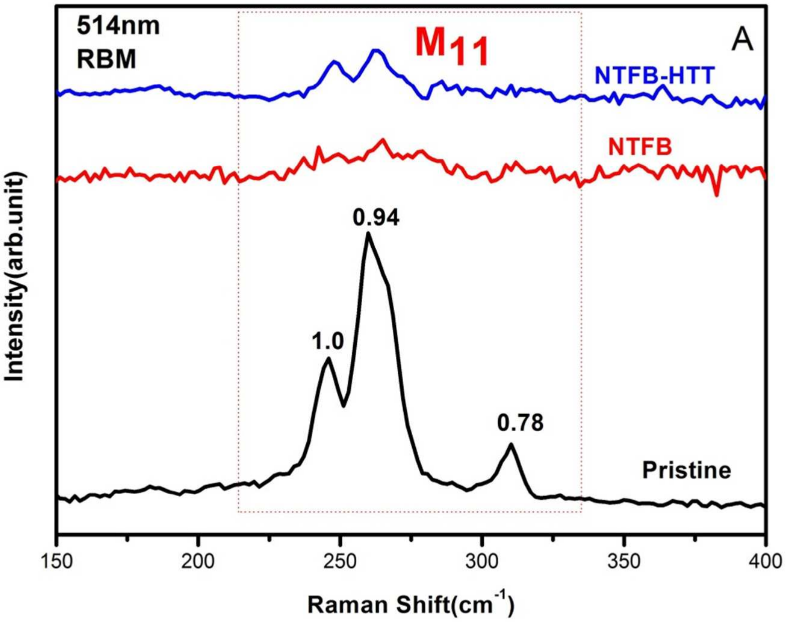
514nm
RBM
M11
A
NTFB-HTT
NTFB
0.94
1.0
0.78
Pristine
Intensity(arb.unit)
150
200
250
300
350
400
Raman Shift(cm-1)

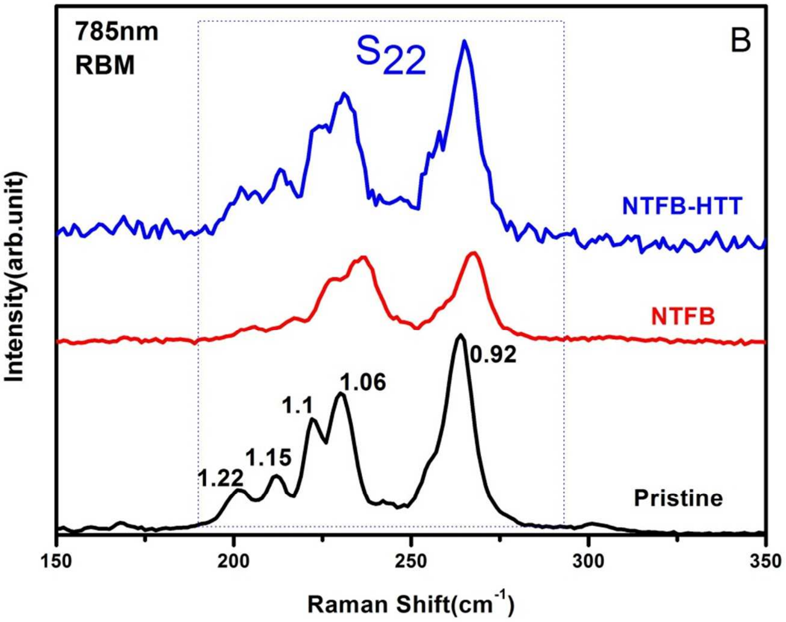
785nm
RBM
S22
B
NTFB-HTT
NTFB
0.92
1.06
1.1
1.15
1.22
Pristine
Intensity(arb.unit)
150
200
250
300
350
Raman Shift(cm-1)

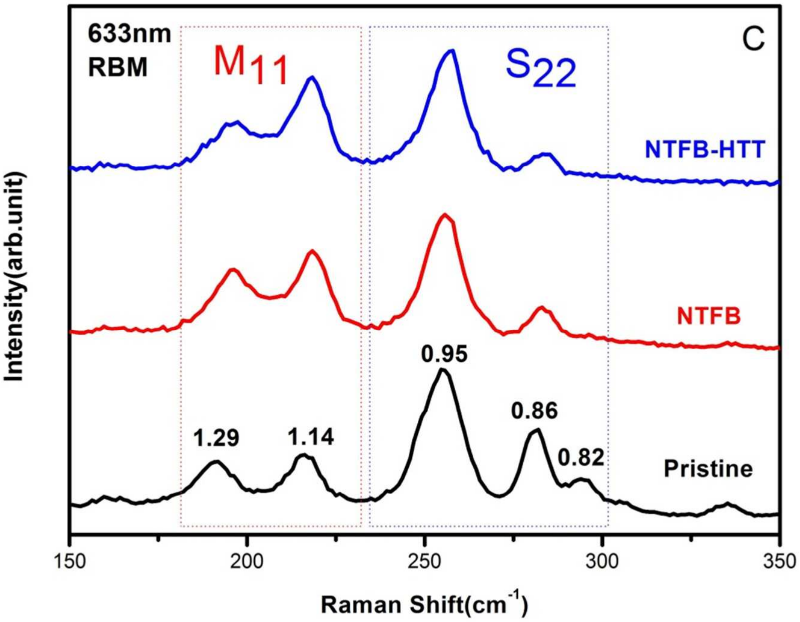

Fig. 1 RBMs of Raman spectra with excitation energies of 514 nm (A), 785nm (B), and 633nm (C) for the pristine sample, the NTFB treated sample, and the NTFB-HTT sample.

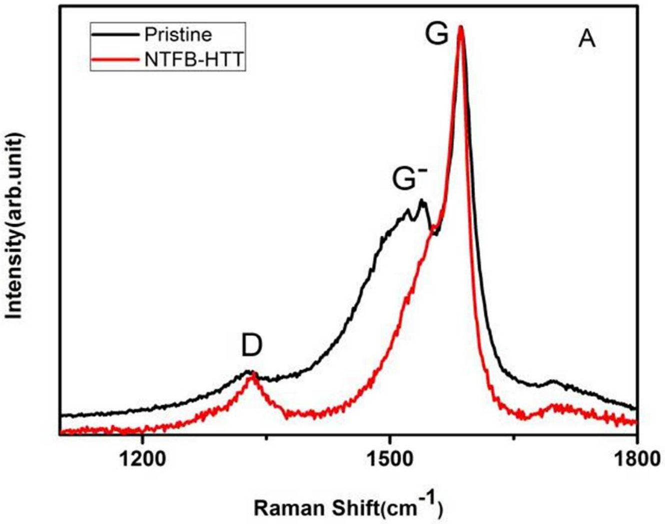

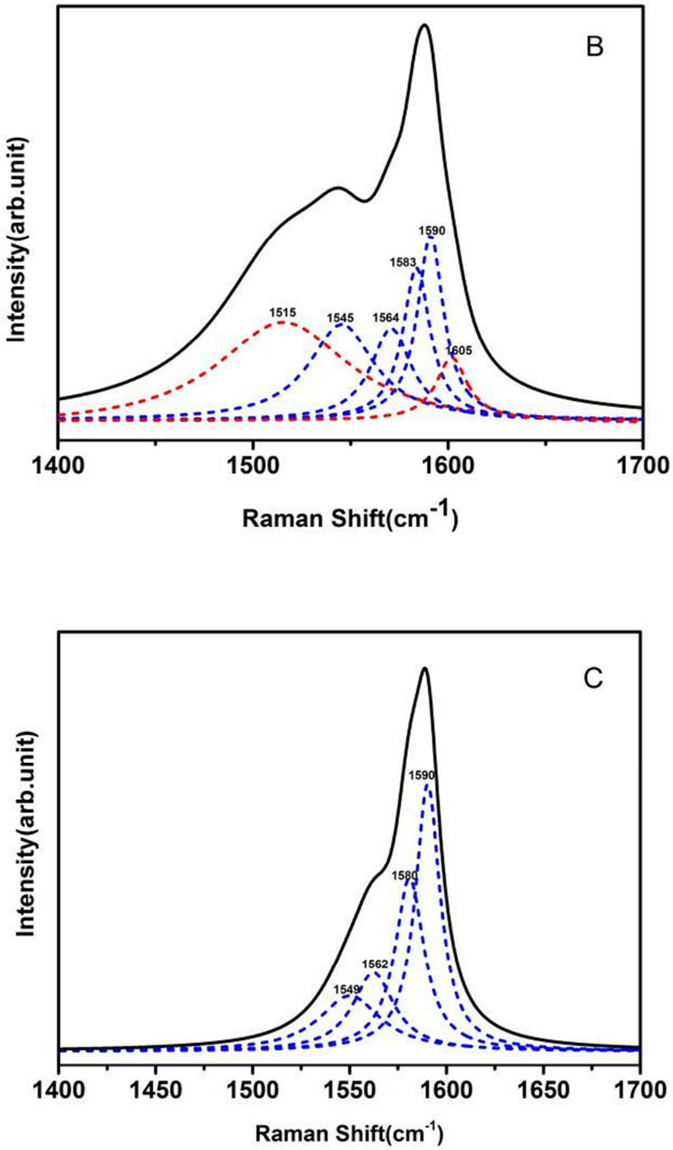

Fig. 2 G and D bands of resonant Raman spectra for the SWCNT samples measured using excitation wavelength of 514 nm (A). Lorentzian curve fitting of the G band for pristine SWNTs, in which four semiconducting Lorentzian line shapes and two metallic BWF line shapes (red color) can be observed (B). Lorentzian curve fitting of G band for the NTFB-HTT SWCNTs, where only four semiconducting Lorentzian line shapes are identified (C)

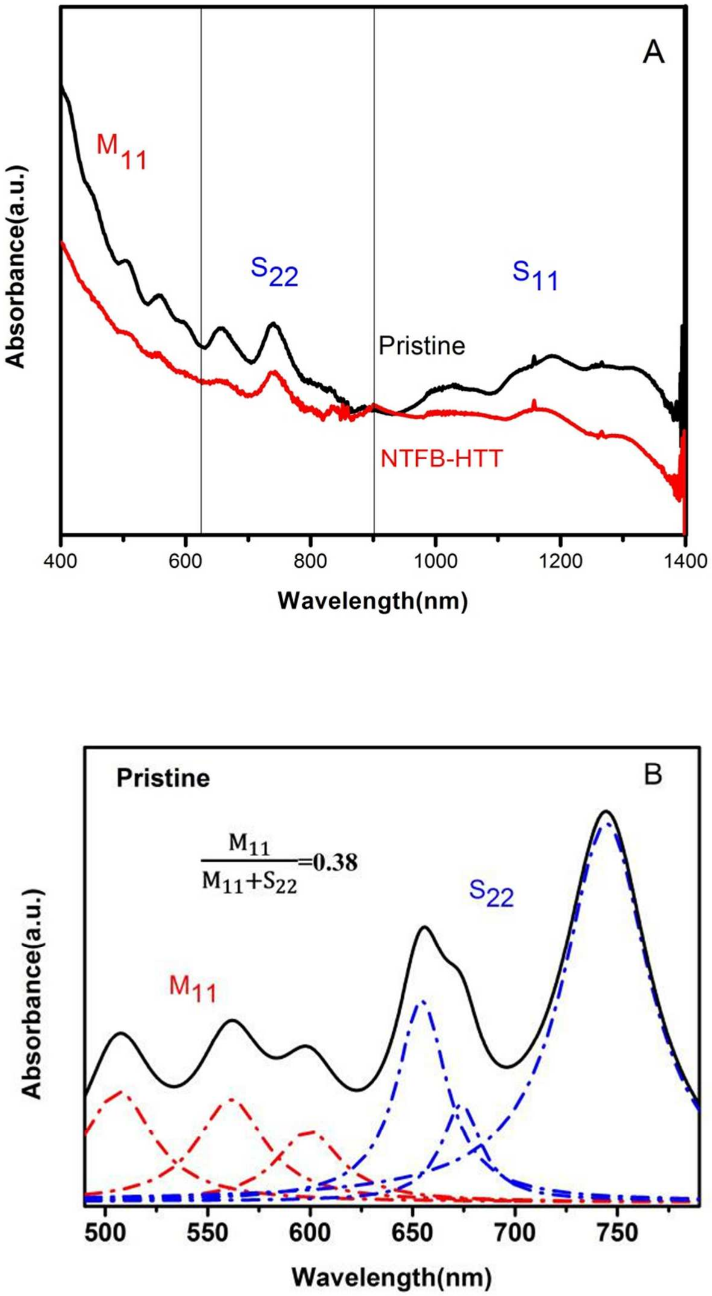
A
M11
S22
S11
Pristine
NTFB-HTT
Absorbance(a.u.)
400
600
800
1000
1200
1400
Wavelength(nm)
Pristine
B
M11/(M11+S22)=0.38
S22
M11
Absorbance(a.u.)
500
550
600
650
700
750
Wavelength(nm)

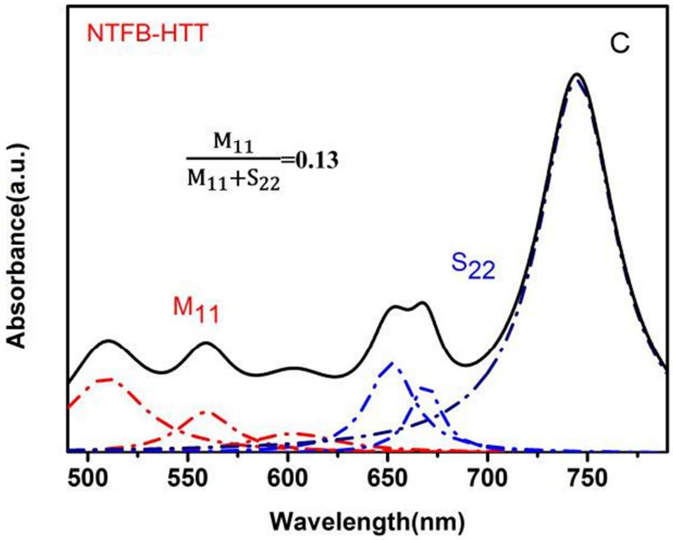

Fig. 3 UV-vis-NIR spectra of the pristine and the NTFB-HTT samples (A), the Lorentzian curve fitting spectra for the pristine sample (B) and the NHFA-HTT sample (C)

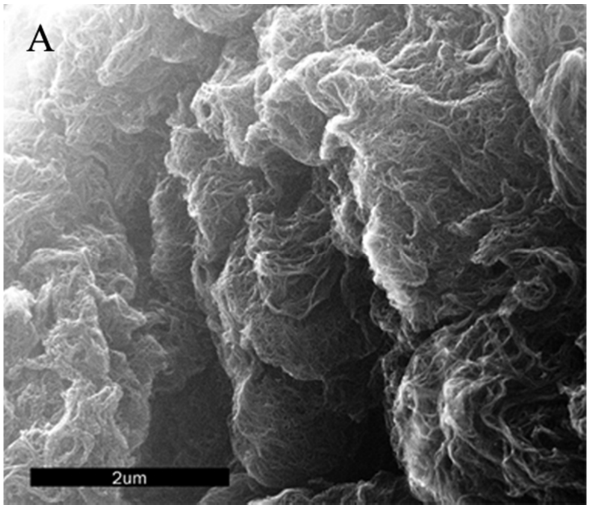

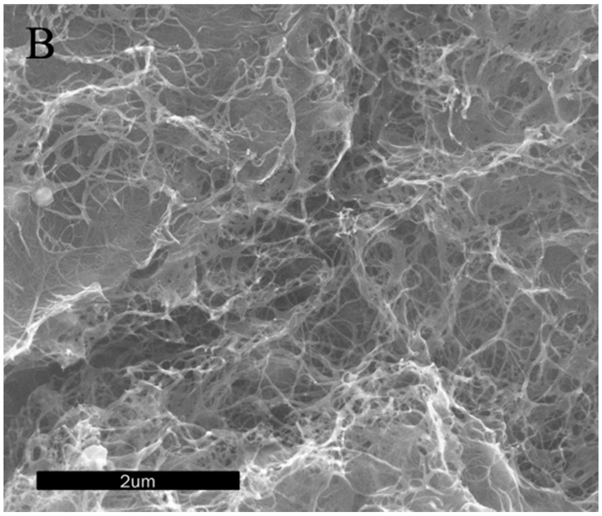

Fig. 4 SEM images of the pristine sample (A) and the NTFB-HTT sample (B)

Table of contents entry

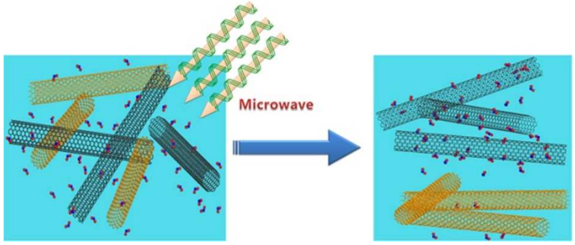

The synergistic effect of microwave irradiation and nitronium ions selective attack made the separation of S-SWCNTs from the counterparts more efficient.